Neural network approach to output updating for the physically-based model of the Upper Thames River watershed

Ponselvi Jeevaragagam

Faculty of Civil Engineering,
Universiti Teknologi Malaysia,
Skudai 81310, Johor Bahru, Johor, Malaysia
E-mail: ponselvi@utm.my

Slobodan P. Simonovic*

Department of Civil and Environmental Engineering,
University of Western Ontario,
London, Ontario N6A 5B9, Canada
E-mail: simonovic@uwo.ca
*Corresponding author

Abstract: This study presents an output updating procedure for the deterministic physically-based model of the Upper Thames River watershed, Ontario, Canada. In addition to streamflow and rainfall, this procedure uses as inputs meteorological variables not employed in the model calibration. The main hydrological processes involved in transformation of rainfall into runoff are mathematically expressed using a set of key variables. Therefore, some of the available meteorological variables may be of limited value during the calibration that predominantly relies on a large range of flow hydrographs for obtaining the optimum state variables and parameters of the model. In this study, the Bayesian regularisation neural network technique is coupled with the physically-based model to provide more accurate flood flow simulation for a wide range of flood flow event hydrographs pertinent to the hydrometeorological environment. The artificial neural network is capable of generating good generalisation results after complex input-output mapping.

Keywords: neural networks; ungauged watershed; streamflow improvement; flood flow event hydrograph; climates; rainfall; hydrologic model; Canada.

Reference to this paper should be made as follows: Jeevaragaga, P. and Simonovic, S.P. (2012) 'Neural network approach to output updating for the physically-based model of the Upper Thames River watershed', *Int. J. Hydrology Science and Technology*, Vol. 2, No. 3, pp.306–324.

Biographical notes: Ponselvi Jeevaragagam is a Senior Lecturer at the Faculty of Civil Engineering, Universiti Teknologi Malaysia. Her research focuses on hydrology and water resources engineering.

Slobodan P. Simonovic is a Professor at the Department of Civil and Environmental Engineering, University of Western Ontario and the Director of Engineering Studies with the Institute for Catastrophic Loss Reduction. His primary research interest focuses on the application of systems approach to, and development of the decision support tools for, management of complex water

Copyright © 2012 Inderscience Enterprises Ltd.

and environmental systems. Most of his work is related to the integration of risk, reliability, uncertainty, simulation and optimisation in hydrology and water resources management. He has received a number of awards for excellence in teaching, research and outreach. He has published over 350 professional publications and two major textbooks.

1 Introduction

The hydrometeorological observations and a rainfall-runoff model are the most fundamental elements of any study of streamflow prediction in a watershed. For example, they provide flood warning messages that are of high importance for the safety of people and protection of property. Hydrometeorological observations include streamflow, precipitation, and various meteorological data. The rainfall-runoff model may use some of the hydrometeorological data in the simulation of hydrological processes to produce flow hydrograph as output. Rainfall-runoff modelling can be done using either an empirical, conceptual or physically-based model. According to the spatial distribution of hydrologic parameters, these models can be lumped, semi-distributed or distributed (Beven, 2001; Cunderlik, 2003). In most studies, the deterministic physically-based models use mathematical representations to describe the selected hydrological processes, as well as a number of state variables and also parameters of the model. Model calibration, using a large number of time series observation data provides values for model parameters. However, models may not be ideal for accurately simulating flow for a wide range of hydrometeorological conditions. Furthermore, the output error(s) from gauged location(s) of physically-based model can cause a significant input error(s) at ungauged location(s). This output error may result from the model limitations:

1 model structure

2 time variation

3 insufficient data; and other factors.

The output error of a deterministic physically-based model can be reduced by implementing an updating procedure based on the artificial neural network (ANN) technique. Neural network is a sophisticated technique, capable of learning the relationships between inputs and outputs without analysing the internal structure of the hydrological processes.

The neural network technique is widely used in hydraulics and hydrology. A few studies have been conducted to review the theory and applications of the ANN in hydrology (ASCE, 2000; Govindaraju and Rao, 2000). Previous studies have demonstrated that ANNs are appropriate for modelling non-linear relationships of rainfall-runoff processes (Zealand et al., 1999; Lekkas et al., 2004; Rajurkar et al,. 2004; Ahmad and Simonovic, 2005; Cullmann et al., 2006); stream-flow forecasting (Anctil et al., 2004; Moradkhani et al., 2004); river stage forecasting (Thirumalaiah and Deo, 1998; Bhattacharya and Solomatine, 2000; Liong et al., 2000); evapotranspiration prediction (Eslamian et al., 2012). The research has been reported to include meteorological data (such as, air temperature, snowmelt, relative humidity, evapotranspiration, wind direction, etc.) to improve the ANN prediction (Poff et al.,

1996; Anctil and Rat, 2005; Jain and Srinivasulu, 2006; Wardah et al., 2008; Aytek et al., 2008). There are many different updating approaches available in the hydrologic literatures that are most appropriate for the study of rainfall-runoff processes in the gauged watersheds (Xiong and O'Connor, 2002; Anctil et al., 2003; Abebe and Price, 2004; Xiong et al., 2004; Goswami et al., 2005; Abrahart and See, 2007). It was found that various input-output combinations of observations and/or simulated results used in these procedures could reduce the associated uncertainty, and improve the overall efficiency of the hydrological model. The most common updating approaches include: use of optimisation methods in the ANN weight updates; use of output error of a physically-based model in the streamflow forecasting; emulation of hydrological knowledge in a numerical model; and the development of a hybrid system coupled by two (or more) linear and/or non-linear models.

In the presented work, a new updating approach is introduced to obtain the most accurate streamflow values at the ungauged sites, through improving the computed streamflow of the hydrologic model at the gauged sites with the assistance of ANN model using available additional hyrometeorological. The results of the study could be helpful in the reduction of flood damages and could allow for safer operation of reservoirs and more effective water resources management.

The paper starts with the presentation of a model output updating methodology in the next section. The implementation of the methodology to the Upper Thames River basin follows. The paper ends with the presentation of results and conclusions obtained from the study.

2 A model output updating methodology

The calibration of hydrologic model, which consists of a number of gauged and ungauged sub-watersheds, is a time-consuming process. It can be done automatically and/or manually. The model calibration process is conducted manually by Cunderlik and Simonovic (2004). The parameters of the model obtained in that way did not make physical sense and therefore, a manual procedure was used to arrive at the model parameters. The calibration started with the most upstream sub-watersheds first and then proceeded downstream. As the process moved downstream numerous iterations were required to re-calibrate the upstream sub-watersheds.

The study presented in this paper introduces a new procedure based on the ANN approach for reducing the output error of a deterministic physically-based model. One of the main advantages of this procedure is the inclusion of additional real-time data on the hydrometeorological environment. While the additional real-time data is not used in the model calibration, it is used by ANN model to provide more accurate flow values for a wide range of flow hydrographs. Other advantages of this procedure are that it requires less computation time and provides more accurate updates for the output flow of the physically-based model for both recent and future flow hydrographs. Furthermore, the output flow at the ungauged streamflow sites can be improved using the updated flow at the corresponding gauged streamflow sites. The information on the updated flow hydrographs at the gauged and/or ungauged streamflow sites can be used in water resources management. For example, the information on flow can be used to reduce the flood damages, and allow for safer operation of reservoirs and other water resources infrastructure.

The overall procedure of output updating of the physically-based model, as illustrated in Figure 1, is presented next. First, the physically-based model is run by using input variables to compute the flow values. Next, the neural network model, ANN1, is applied by using available hydrometeorological observation data to improve the output flow of the physically-based model for the selected gauged streamflow sites in a watershed. The improved flows of the gauged sites as well as the hydrometeorological data are then used by the second neural network model, ANN2, to update the computed flow values of the physically-based model for the corresponding ungauged sites. The steps in the proposed methodology based on the computational engine of the HEC-HMS (USACE, 2000) are summarised as follows:

1 Determine the computed streamflow at the gauged site of the HEC-HMS model, $Q_{gHMS}(t)$.

2 Estimate the improved streamflow(s) at the gauged site(s), $iQ_{gHMS}(t)$, using the neural network model (ANN1), as given by:

$$iQ_{gHMS}(t) = Q_{gANN}(t) \tag{1}$$

$$Q_{gANN}(t) = f\begin{pmatrix} QgHMS(t-1);\ Q_o(t-1); \\ \text{and other available meteorological data} \end{pmatrix} \tag{2}$$

where in the training process the ANN1 model's target output is the observed streamflow of the gauged site, $Q_o(t)$. The computed streamflow ($Q_{gHMS}(t)$) is improved with the assistance of the ANN approach. The simulated flow generated by the ANN model (ANN1), $Q_{gANN}(t)$ using equation (2), becomes the improved streamflow at the gauged site, $iQ_{gHMS}(t)$ according to equation (1). The previous and/or recent HEC-HMS computed streamflow of gauged site, observed streamflow, mean-areal rainfall, and additional meteorological variables are used by the ANN model (ANN1) in the output updating procedure.

3 Improve the model calculated streamflow values at the corresponding ungauged sites, by using the neural network model (ANN2), as follows:

$$iQ_{ugHMS}(t) = Q_{ugANN}(t) \tag{3}$$

$$Q_{ugANN}(t) = f\begin{pmatrix} \sum_{i=1}^{G} Q_{gHMS,i}(t);\ Q_{ugHMS}(t-1);\ Q_o(t-1); \\ \text{and other available meteorological data} \end{pmatrix},\ i = 1, 2, \ldots\ldots, G \tag{4}$$

where f is the ANN function of input-output datasets, $Q_{gHMS}(t)$ and $Q_{ugHMS}(t)$ are the HEC-HMS computed flows at the gauged and ungauged sites, respectively; $Q_o(t-1)$ is an average observed flow at the gauged site; $iQ_{gHMS}(t)$ is the improved streamflow(s) from the gauged site(s) for G gauging sites; $iQ_{ugHMS}(t)$ is the improved streamflow at the ungauged site; and $t = 1$ to N is the time step. The ANN2 model's target output in the training process is $Q_{ugHMS}(t)$.

4 Test the ANN2 model with the improved streamflow of gauged site(s), $iQ_{gHMS}(t)$ obtained from equations (1) and (2), instead of using the $Q_{gHMS,i}(t)$ in equation (4).

The ANN simulated streamflow, $Q_{ugANN}(t)$, is then compared with the streamflow observation from the ungauged site.

Figure 1 Schematic diagram of the output updating procedure

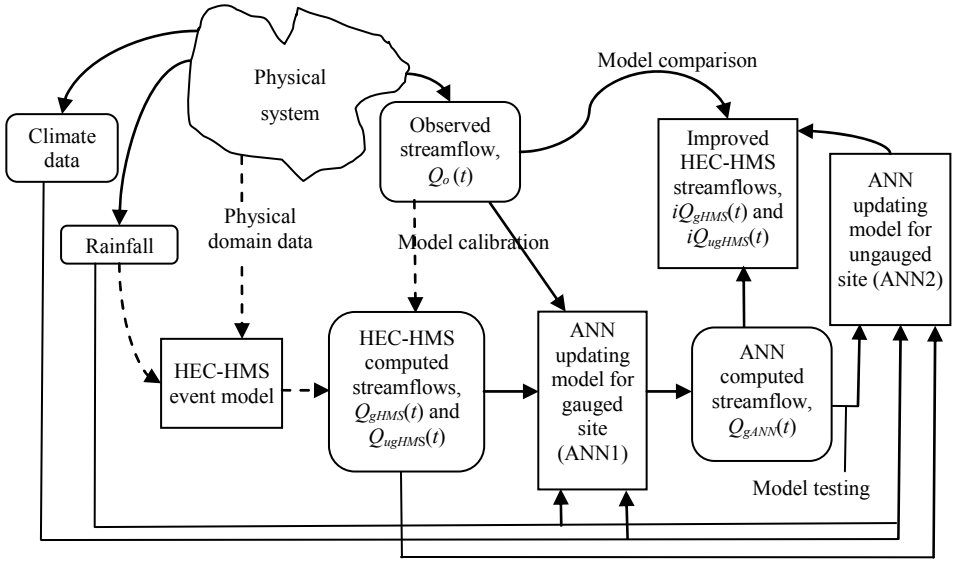

In the next section, the Levenberg-Marquardt (LM) algorithm with Bayesian regularisation, and the model evaluation criteria used with the presented methodology are discussed in detail.

2.1 The LM algorithm with Bayesian regularisation

The Bayesian regularisation neural network is a more recent technique that can ensure accurate prediction of flow values, while automatically preventing the overfitting and underfitting when the network is tested with unknown inputs. Other advantage of this approach is that during training it applies an early stopping procedure as soon as the overtraining signal starts to appear. The overtraining signal can be observed when the trained network is tested with an unknown dataset and the obtained output has a higher accuracy. The Bayesian regularisation uses either training, or validation or both datasets to learn all ranges of possible datasets, which is especially valuable when the size of the dataset is small. In many examples, a multilayer feed-forward network with the LM algorithm has proven to be faster and more effective in finding optimal results (Masters, 1995; Bertsekas and Tsitsiklis, 1996; Tan and Van Cauwenberghe, 1999; Anctil et al., 2003). According to Hagan and Menhaj (1994), the LM algorithm belongs to the category of second-order non-linear optimisation techniques. The performance of ANN model in this study is found superior when the Bayesian regularisation is used with LM algorithm in training the multilayer feed-forward network (Foresee and Hagan, 1997; Anctil et al., 2003; Parent et al., 2008). This study has applied a multilayer feed-forward network with a single hidden sigmoid and linear output layer.

In the Bayesian framework, a term that consists of mean of the sum of squares of the network weights and biases, F_w, is automatically added, to the typical error function (the

mean sum of squares of the network errors), F_e, to improve generalisation, as given in the following (MacKay, 1992):

$$F = \beta F_e + \alpha F_w = \beta \sum_{i=1}^{N} e_i^2 + \alpha \sum_{i=1}^{M} W_i \tag{5}$$

where F is the error function; e, is the network error, the difference between the desired flow, Q_o, and the network output, Q_{gANN} or Q_{ugANN} for N number of training inputs; W is the network weight and bias for M total number of weights; α and β are the error function parameters. The algorithm steps for training the ANN model are as follows:

1 Initialise the error function parameters, α and β, and the weights (Nguyen and Widrow, 1990).

2 Present all inputs of size N to the network, and compute the network errors, e. Then, compute the error function, F, over all inputs using equation (5).

3 Take one step of the LM algorithm to minimise the error function.

4 Compute the Hessian matrix, **H**, and the gradient, **g**, using the Jacobian matrix, **J**, that contains the first derivatives of the network errors with respect to the weights and biases, as follows:

$$\mathbf{H} = \frac{\partial^2 F}{\partial w^2} = \mathbf{J}^T \ \mathbf{J} \tag{6}$$

$$\mathbf{g} = \frac{\partial F}{\partial w} = \sum \frac{\partial e}{\partial w} \mathbf{e} = \mathbf{J}^T \mathbf{e} \tag{7}$$

5 Compute the parameters with new values, $\alpha = \gamma / (2F_w)$ and $\beta = (N - \gamma) / (2F_e)$, using the value of the effective number of parameters $\gamma = N - 2\alpha \mathrm{tr}(\mathbf{H})^{-1}$.

6 Solve the ANN weight, using the LM update given in the following:

$$\mathbf{W}_{k+1} = \mathbf{W}_k - \mathrm{D}\mathbf{W} = \mathbf{W}_k - [\mathbf{H} + \mu \mathbf{I}]^{-1} \mathbf{g} \tag{8}$$

where $\Delta\mathbf{W}$ is the updated weight, $\mathbf{W}_k$ is the weight matrix at training iteration (k), **I** is the identity matrix, and μ is a scalar that controls the learning process.

7 Recompute the error function, F_{k+1}, using equation (5) and the new weight W_{k+1} obtained in step 6. If the new error is reduced ($F_{k+1} < F_k$), then LM algorithm decreases the μ by μ^-, the new weight Wk+1 is calculated, and the process starts again from step 2; otherwise, the algorithm increases the μ by μ+, and the weight of ΔW from step 6 is recalculated; The default values of μ+ = 10 and μ– = 0.1 are usually used.

8 The training procedure is considered to converge when the effective number of parameters, γ, has converged, or the error is reduced up to some predefined error goal.

2.2 Model evaluation criteria

The performance predictions of the ANN model and physically-based model at the gauged streamflow location are evaluated for training, validation and testing datasets. The general performance of ANN predictions with is evaluated using the correlation coefficient of linear regression, R, in equation (9), between computed and observed streamflows. A high number of R = 1.0 means perfect statistical correlation and a low number of R = 0.0 means there is no correlation at all. The success measurement of sensitivity analysis for choosing the input variables is based on the root mean square error (RMSE), given by equation (10), which measures the level of fitness between the ANN model output and the observed data. This measure ignores the importance of low and high flows (Coulibaly et al., 2001). The peak flow criterion (PFC) in equation (11), is used to identify the more accurate ANN model for flood flow simulation. The mean absolute error (MAE), given by equation (12), measures the average of the absolute error value (the difference between the observed data and the model predicted output). The MAE is similar to the RMSE, but they differ in their weighting of the errors. Lower values of RMSE, PFC and MAE indicate a good model fit to the observation data. The correlation between the predicted hydrograph and the observed hydrograph is evaluated using the Nash-Sutcliffe coefficient of efficiency (Nash and Sutcliffe, 1970), EI, given by equation (13), which ranges from negative infinity to 1.0. An EI value of 1.0 means a perfect agreement between the observed and predicted hydrographs. The EI value equal to, or less than 0.0, indicates that the one-parameter 'no knowledge' model is better than simulation model output. In this case, the observed hydrograph is suggested as a better predictor than the simulated one. The flow volume error (FVE), given by equation (14), only considers the computed flow volume and does not account for the magnitude or timing of the peak flow. The 0.0 value of FVE means a perfect agreement of flow volume. Conversely, a negative value of FVE means the simulated flow is slightly under predicted in comparison to the volume of observed flow. Finally, both observed and predicted flow hydrographs for the testing dataset are plotted for visual evaluation.

$$\mathrm{R} = \frac{\sum_{t=1}^{N}\left(Q_t - Q_{ave}\right)\left(\hat{Q}_t - \hat{Q}_{ave}\right)}{\sqrt{\sum_{t=1}^{N}\left(Q_t - Q_{ave}\right)^2\left(\hat{Q}_t - \hat{Q}_{ave}\right)^2}} \tag{9}$$

$$\mathrm{RMSE} = \left[\frac{1}{N}\sum_{t=1}^{N}\left(Q_t - \hat{Q}_t\right)^2\right]^{1/2} \tag{10}$$

$$\mathrm{PFC} = \frac{\left(\sum_{t=1}^{NP}\left(Q_t - \hat{Q}_t\right)^2 Q_t^2\right)^{1/4}}{\left(\sum_{t=1}^{NP} Q_t^2\right)^{1/2}} \tag{11}$$

$$\mathrm{MAE} = \frac{1}{N}\sum_{t=1}^{N}\left|Q_t - \hat{Q}_t\right| \tag{12}$$

$$\mathrm{EI} = 1 - \frac{\sum_{t=1}^{N}\left(Q_t - \hat{Q}_t\right)^2}{\sum_{t=1}^{N}\left(Q_t - Q_{ave}\right)^2} \tag{13}$$

$$\mathrm{FVE} = \frac{\sum_{i=1}^{N} Q_t - \sum_{i=1}^{N}\hat{Q}_t}{\sum_{i=1}^{N} Q_t} \tag{14}$$

where $\hat{Q}$ is the ANN predicted streamflow for the gauged or ungauged location, Q is the observed streamflow or HEC-HMS computed flow for the ungauged location at t, recent time step, Q_{ave} is the average streamflow; N is the number of observations, and NP is the number of peak flows greater than one-third of the mean peak flow.

3 Case study

3.1 The input data for output updating

The proposed methodology for output updating of the physically-based model is presented using the study of the Upper Thames River watershed, located in southwestern Ontario, Canada. The watershed is comprised of four counties: Perth, Middlesex, Huron and Oxford. This study uses five events during the periods 2000 and 2004. The hourly meteorological data from the nearest monitoring sites, such as Stratford (solar radiation), Wildwood Dam (evaporation) and London (air temperature, wind speed, wind direction, air station pressure, visibility, and humidity) are used in the updating procedure. These hourly historic datasets are obtained from the Environment Canada (EC) and the Upper Thames River Conservation Authority (UTRCA). One gauged streamflow location, St. Marys, is selected to illustrate the methodology for output updating of the HEC-HMS event hydrologic model of the Upper Thames River watershed. The improved streamflow from this gauged site is used in the ANN model to determine the streamflow value for the ungauged site, Plover Mills (see Figure 2). The St. Marys SG is a gauged site, and Plover Mills SG in Figure 2 is considered as an ungauged site. Available observations at Plover Mills SG are used at the end to check the quality of streamflow forecast for ungauged sites. In other words, we artificially treated the Plover Mills Sg as ungauged. Data and analyses for other stations in the watershed are available from the first author upon request.

A more detailed description of the Upper Thames River watershed and the HEC-HMS hydrologic model follows.

Figure 2 HEC-HMS event hydrologic model of the Upper Thames River watershed (see online version for colours)

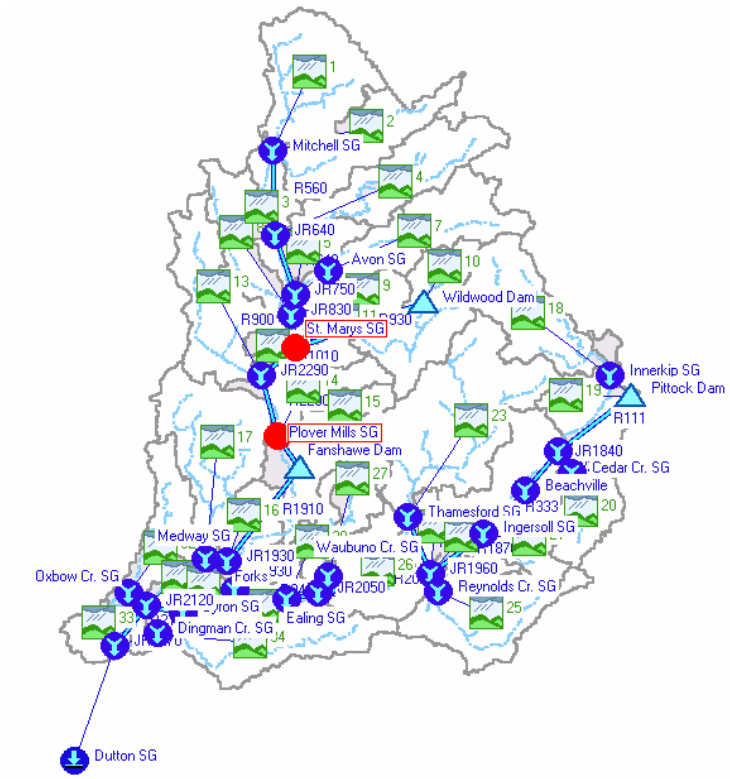

3.1.1 Description of the Upper Thames River watershed

There are two main tributaries of the Thames River: the North branch (1,750 km^2) and the East branch (1,360 km^2). They converge at forks near the centre of the city of London. The Thames River then flows westwards and exits the outlet of watershed near Byron. The watershed receives 1,000 mm of annual precipitation with an estimated annual discharge of 35.9 m^3/s (measured at Byron station). About 60% of the annual precipitation is lost through evaporation and/or evapotranspiration, accumulated water in ponds and wetlands, or infiltration. The slope at the upper reaches of the Thames basin is close to 1.9 m/km and much flatter at lower reaches – less than 0.2 m/km (Wilcox et al., 1998). The Thames River flows are attenuated by three major reservoirs, Wildwood, Fanshawe and Pittock, all built in the mid-1960s for the purpose of flood management. Since then, the purposes of reservoirs have expanded to low flow maintenance and recreation. The Upper Thames River watershed has historically experienced severe flooding, going as far back as the late 1700s. By the late 1930s and early 1940s, flood events forced the formation of the Conservation Authorities in 1946 to provide solution for problems associated with flooding. The dates of more recent floods in this watershed include March 1977, September 1986, July 2000, April 2008, and December 2008 (UTRCA, 2009). Flooding most frequently occurs after the spring snow melts and summer storms (Prodanovic and Simonovic, 2006).

Figure 3 The event hydrologic model structure

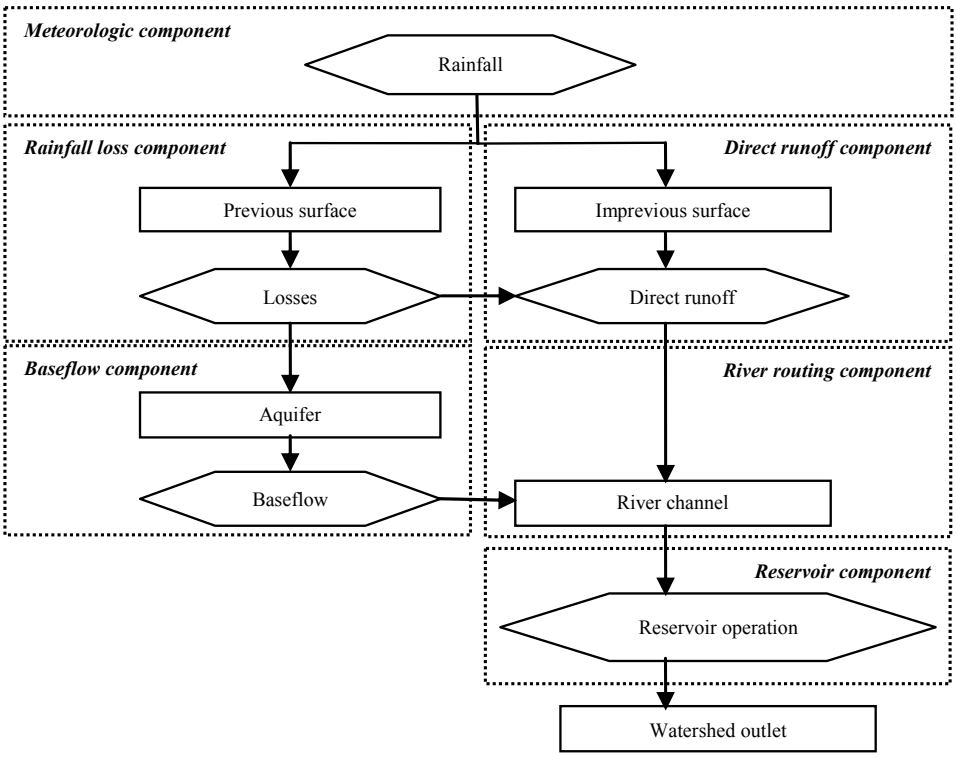

3.1.2 The HEC-HMS event hydrologic model

The rainfall-runoff model for the Upper Thames River watershed was originally developed using the Hydrologic Modeling System (HEC-HMS) version 2.2.2 (USACE, 2000), a product of the Hydrologic Engineering Center within the US Army Corps of Engineers. The details of this work can be found in the report by Cunderlik and Simonovic (2004). The computational engine of HEC-HMS model was later reprogrammed in the Java programming language to speed up the process for performing a large number of simulations. The HEC-HMS hydrologic model for the Upper Thames River watershed, as illustrated in Figure 2, consists of thirty three sub-watersheds, twenty one river reaches, and three reservoirs. The hydrologic model is divided into six main components, each representing the different hydrologic process occurring in the watershed, as shown in Figure 3. In this study, the calibrated HEC-HMS hydrologic model in the Java programming language is used. First, the meteorologic component is used to provide spatially and temporally distributed rainfall over the watershed. The rainfall is then used as the input data in the calibrated HEC-HMS model for estimating the streamflow at the watershed outlet. The rainwater infiltrates either a previous surface or an impervious surface. The rainfall loss component accounts for the water losses through interception, infiltration, evaporation and transpiration, for rainfall from the previous surface. The effective rainfall from the loss component contributes to direct runoff and to groundwater flow in aquifers. Rainfall from the impervious surface is used

by the direct runoff component to generate overland flow. The water moisture movement in aquifers is modelled by the baseflow component. The overland flow and baseflow are then combined to produce streamflow. The river routing component uses the streamflow as input to propagate the flood wave along a river channel. Finally, the effect of hydraulic facilities (reservoirs, and detention basins) and natural depressions is reproduced by the reservoir component.

3.2 The neural network model

The ANN input data used in the network training include the HEC-HMS computed flood flow of gauged site in the previous/current time interval and/or the HEC-HMS computed flood flow of ungauged site in the previous time interval, average flood flow in the previous time interval, total rainfall, and meteorological variables (such as average visibility, average relative humidity, average wind speed, average solar radiation, average air station pressure, average evaporation, average air temperature, and average wind direction) in the current and previous time intervals. The autocorrelation and cross-correlation analyses are performed on the ANN input data, to determine the ANN configuration models. For example, Table 1 shows the best correlation coefficient results (with lag-times from 1 to 10 hours) for St. Marys, Mitchell and Stratford flood flows, total rainfall, and other meteorological variables. The correlation functions are computed with 95% confidence interval.

Table 1 The autocorrelation (A) and cross-correlation (X) results for St. Marys flood flow

Lags	*X(Ws)*	*X(Sr)*	*X(Wd)*	*X(H)*	*X(Sp)*	*X(T)*	*X(V)*	*X(E)*
0	–0.01	–0.10	0.13	0.20	–0.32	0.04	–0.18	–0.16
1	–0.02	–0.10	0.12	0.21	–0.32	0.05	–0.19	–0.16
2	–0.01	–0.10	0.11	0.21	–0.32	0.06	–0.20	–0.16
Lags	*X(R)*	*A(QSm)*	*A(QM)*	*A(QS)*				
0	0.24	1.00	0.85	0.87				
1	0.23	0.99	0.85	0.91				
2	0.23	0.98	0.85	0.93				
3	0.22	0.95	0.84	0.94				
4	0.20	0.92	0.82	0.94				
5	0.19	0.88	0.81	0.92				
6	0.17	0.84	0.78	0.90				
7	0.15	0.80	0.76	0.86				
8	0.12	0.76	0.73	0.83				
9	0.10	0.72	0.70	0.79				
10	0.07	0.68	0.66	0.76				

Notes: Where *QHg* and *QHug* are the computed flood flow of HEC-HMS for St. Marys gauged site and Plover Mills ungauged site, respectively; *QSm*, *QM*, and *QS* are the average flows (m^3/s) at St. Marys, Mitchell, and Stratford stations, respectively; *R* is the total rainfall (mm); *V* is the hourly average visibility (km); *H* is the hourly average relative humidity (%); *Ws* is the hourly average wind speed (km/h); *Sr* is the hourly average solar radiation (MJ m^{-2} $hour^{-1}$); *Sp* is the hourly average air station pressure (kPa); *E* is the hourly average evaporation (mm $hour^{-1}$); *T* is the hourly average air temperature (°C); *Wd* is the hourly average wind direction (10's Deg); and *t* is the recent time and delayed hourly eight times $t-1$, $t-2$, ……, $t-6$ and $t-8$.

From Table 1, the St. Mary, Mitchell and Stratford flows with lag-times of 1- to 2-hour (QSm_{t-1}, QSm_{t-2}, QM_{t-1}, QM_{t-2}, QS_{t-1} and QS_{t-2}); the rainfall with lag-times of 1- to 8-hour (R_{t-1}, R_{t-2}, ….., R_{t-7} and R_{t-8}); and most of other meteorological variables with lag-time of 1-hour (e.g., Sr_{t-1}) are considered as potential candidates correlated with the recent hour St. Marys flow forecast (QSm_t). The development of ANN input configuration models, is presented in the next section.

Based on the results from correlation analysis, different hourly neural network input models are developed that are highly correlated with the recent observed flood flow, as summarised in Table 2 (for St. Marys station selected as an example). Sensitivity analyses are conducted for these input models to determine the optimal input configuration and number of hidden nodes, using the LM algorithm with Bayesian regularisation approach. Tables 3 and 4 show the datasets used in the network training for St. Marys and Plover Mills stations. From Tables 2 and 5 for St. Marys station, the input configuration M20 with visibility and station pressure variables has the minimum RMSE value of 1.54 m^3/s when compared with the model configurations M21 to M26 using other meteorological variables. In the case of M21 to M26, the analyses consider visibility, humidity, wind speed, solar radiation, air station pressure, evaporation, air temperature and wind direction. These variables are not used in the output updating process. Multilayer feed-forward networks with a range of 5 to 15 hidden nodes are successively trained, and the best performance with the test dataset is obtained within a pool of 25 repetitions. This implies that the selected configuration is among the top 14% of the distribution of all possible configurations, with 95% confidence, according to Iyer and Rhinehart (1999). Note that before training, all mean and standard deviation values of the input configurations are constantly normalised. The datasets used for the training, validation and testing a network, as given in Tables 3 and 4 for St. Marys and Plover Mills stations are selected by implementing data cross-validation, extreme data partition, and trial and error methods. The results of sensitivity analyses for the training dataset are given in Table 5 only for the St. Marys station. This result suggests improvement in the RMSE value of the trained network when additional meteorological data is used. For example, for St. Marys station, the optimal input configuration M20 with 15 input variables and nine hidden nodes offers the minimum RMSE value of 1.54 m^3/s for a given training dataset. For Plover Mills station (the results are not shown here) the minimum RMSE value of 1.02 m^3/s is obtained using the training dataset with 17 input variables and 13 hidden nodes. The best ANN input configurations are presented in equations (15) and (16) for St. Marys and Plover Mills stations, respectively.

St. Marys station:

$$Q(t) = \mathrm{f}\begin{pmatrix} QHg(t-1),\ QSm(t-1),\ QS(t-1),\ QM(t-1), \\ QM(t-2),\ R(t-1),\ R(t-2),\ R(t-3), R(t-4), \\ R(t-5), R(t-6),\ R(t-7),\ R(t-8),\ V(t-1) \text{ and } Sp(t-1) \end{pmatrix} \tag{15}$$

Plover Mills station:

$$Q(t) = \mathrm{f}\begin{pmatrix} QHg(t),\ QHug(t-1),\ QHug(t-2),\ QHug(t-3),\ QHug(t-4), \\ R(t-2),\ R(t-3),\ R(t-4),\ R(t-5), R(t-6), R(t-7),\ R(t-8), \\ R(t-9), R(t-10),\ R(t-11),\ R(t-12),\ R(t-13) \end{pmatrix} \tag{16}$$

These trained networks are validated with unknown datasets.

Table 2 ANN input configuration models for the St. Marys station

M1:	QHg_{t-1}, QSm_{t-1} and QSm_{t-2}
M2:	QHg_{t-1}, QSm_{t-1} and QM_{t-1}
M3:	QHg_{t-1}, QSm_{t-1} and QS_{t-1}
M4:	QHg_{t-1}, QSm_{t-1}, QS_{t-1} and QS_{t-2}
M5:	QHg_{t-1}, QSm_{t-1}, QS_{t-1} and QM_{t-1}
M6:	QHg_{t-1}, QSm_{t-1}, QS_{t-1}, QM_{t-1} and QM_{t-2}
M7:	QHg_{t-1}, QSm_{t-1}, QS_{t-1}, QM_{t-1}, QM_{t-2}, R_{t-1}, R_{t-2}, R_{t-3}, R_{t-4}, R_{t-5}, R_{t-6}, R_{t-7} and R_{t-8}
M8:	QHg_{t-1}, QSm_{t-1}, QS_{t-1}, QM_{t-1}, QM_{t-2}, R_{t-1}, R_{t-2}, R_{t-3}, R_{t-4}, R_{t-5}, R_{t-6} and R_{t-7}
M9:	QHg_{t-1}, QSm_{t-1}, QS_{t-1}, QM_{t-1}, QM_{t-2}, R_{t-1}, R_{t-2}, R_{t-3}, R_{t-4}, R_{t-5} and R_{t-6}
M10:	QHg_{t-1}, QSm_{t-1}, QS_{t-1}, QM_{t-1}, QM_{t-2}, R_{t-1}, R_{t-2}, R_{t-3}, R_{t-4} and R_{t-5}
M11:	QHg_{t-1}, QSm_{t-1}, QS_{t-1}, QM_{t-1}, QM_{t-2}, R_{t-1}, R_{t-2}, R_{t-3} and R_{t-4}
M12:	QHg_{t-1}, QSm_{t-1}, QS_{t-1}, QM_{t-1}, QM_{t-2}, R_{t-1}, R_{t-2}, R_{t-3}, R_{t-4}, R_{t-5}, R_{t-6}, R_{t-7}, R_{t-8} and T_{t-1}
M13:	QHg_{t-1}, QSm_{t-1}, QS_{t-1}, QM_{t-1}, QM_{t-2}, R_{t-1}, R_{t-2}, R_{t-3}, R_{t-4}, R_{t-5}, R_{t-6}, R_{t-7}, R_{t-8} and E_{t-1}
M14:	QHg_{t-1}, QSm_{t-1}, QS_{t-1}, QM_{t-1}, QM_{t-2}, R_{t-1}, R_{t-2}, R_{t-3}, R_{t-4}, R_{t-5}, R_{t-6}, R_{t-7}, R_{t-8} and Sr_{t-1}
M15:	QHg_{t-1}, QSm_{t-1}, QS_{t-1}, QM_{t-1}, QM_{t-2}, R_{t-1}, R_{t-2}, R_{t-3}, R_{t-4}, R_{t-5}, R_{t-6}, R_{t-7}, R_{t-8} and Ws_{t-1}
M16:	QHg_{t-1}, QSm_{t-1}, QS_{t-1}, QM_{t-1}, QM_{t-2}, R_{t-1}, R_{t-2}, R_{t-3}, R_{t-4}, R_{t-5}, R_{t-6}, R_{t-7}, R_{t-8} and Wd_{t-1}
M17:	QHg_{t-1}, QSm_{t-1}, QS_{t-1}, QM_{t-1}, QM_{t-2}, R_{t-1}, R_{t-2}, R_{t-3}, R_{t-4}, R_{t-5}, R_{t-6}, R_{t-7}, R_{t-8} and V_{t-1}
M18:	QHg_{t-1}, QSm_{t-1}, QS_{t-1}, QM_{t-1}, QM_{t-2}, R_{t-1}, R_{t-2}, R_{t-3}, R_{t-4}, R_{t-5}, R_{t-6}, R_{t-7}, R_{t-8} and Sp_{t-1}
M19:	QHg_{t-1}, QSm_{t-1}, QS_{t-1}, QM_{t-1}, QM_{t-2}, R_{t-1}, R_{t-2}, R_{t-3}, R_{t-4}, R_{t-5}, R_{t-6}, R_{t-7}, R_{t-8} and H_{t-1}
M20:	QHg_{t-1}, QSm_{t-1}, QS_{t-1}, QM_{t-1}, QM_{t-2}, R_{t-1}, …, R_{t-7}, R_{t-8}, V_{t-1} and Sp_{t-1}
M21:	QHg_{t-1}, QSm_{t-1}, QS_{t-1}, QM_{t-1}, QM_{t-2}, R_{t-1}, …, R_{t-7}, R_{t-8}, V_{t-1}, Sp_{t-1} and H_{t-1}
M22:	QHg_{t-1}, QSm_{t-1}, QS_{t-1}, QM_{t-1}, QM_{t-2}, R_{t-1}, …, R_{t-7}, R_{t-8}, V_{t-1}, Sp_{t-1}, H_{t-1} and E_{t-1}
M23:	QHg_{t-1}, QSm_{t-1}, QS_{t-1}, QM_{t-1}, QM_{t-2}, R_{t-1}, …, R_{t-7}, R_{t-8}, V_{t-1}, Sp_{t-1}, H_{t-1}, E_{t-1} and Wd_{t-1}
M24:	QHg_{t-1}, QSm_{t-1}, QS_{t-1}, QM_{t-1}, QM_{t-2}, R_{t-1}, …, R_{t-7}, R_{t-8}, V_{t-1}, Sp_{t-1}, H_{t-1}, E_{t-1}, Wd_{t-1} and Sr_{t-1}
M25:	QHg_{t-1}, QSm_{t-1}, QS_{t-1}, QM_{t-1}, QM_{t-2}, R_{t-1}, …, R_{t-7}, R_{t-8}, V_{t-1}, Sp_{t-1}, H_{t-1}, E_{t-1}, Wd_{t-1}, Sr_{t-1} and T_{t-1}
M26:	QHg_{t-1}, QSm_{t-1}, QS_{t-1}, QM_{t-1}, QM_{t-2}, R_{t-1}, …, R_{t-7}, R_{t-8}, V_{t-1}, Sp_{t-1}, H_{t-1}, E_{t-1}, Wd_{t-1}, Sr_{t-1}, T_{t-1} and Ws_{t-1}

Table 3 The comparison of performance predictions between the ANN model and the HEC-HMS model for St. Marys gauged site

Dataset and period	*Mean flow (m^3/s)*	*Simulated model*	*RMSE (m^3/s)*	*FVE*	*MAE (m^3/s)*	*EI*	*PFC*	*R*
Training (July and August 2000; May 2004)	70.91	HMS	43.566	0.021	26.516	0.777	0.144	0.888
		ANN	1.591	0.001	0.859	1.000	0.029	1.000
Validation (September 2000)	38.34	HMS	25.173	–0.148	13.325	0.420	0.336	0.951
		ANN	1.482	–0.006	0.763	0.998	0.076	0.999
Test (June 2000)	30.95	HMS	39.654	–0.895	28.608	–1.844	0.371	0.847
		ANN	1.686	–0.010	0.992	0.995	0.076	0.998

Table 4 The performance predictions of the ANN model for Plover Mills ungauged site

Dataset and period	*Mean flow (m^3/s)*	*RMSE (m^3/s)*	*FVE*	*MAE (m^3/s)*	*EI*	*PFC*	*R*
Training (July and August 2000; May 2004)	94.31	0.537	–0.001	0.333	1.000	0.012	1.000
Validation (September 2000)	61.79	0.780	–0.002	0.343	1.000	0.036	1.000
Test (June 2000) – HEC-HMS computed flow	60.44	29.470	0.296	20.171	0.595	0.268	0.888
Test (June 2000) – observed flow	42.74	1.385	0.004	0.617	0.998	0.057	0.999

Table 5 The RMSE (m^3/s) performance results of the ANN network configuration sensitivity analysis for St. Mary station

Models	*Number of hidden nodes*										
	5	*6*	*7*	*8*	*9*	*10*	*11*	*12*	*13*	*14*	*15*
M1	4.72	4.50	4.05	4.47	4.04	4.24	3.86	3.96	4.29	4.09	3.95
M2	8.55	8.33	8.81	8.51	8.61	8.69	8.60	8.07	8.72	8.74	8.75
M3	4.05	3.72	4.36	4.26	3.91	4.49	4.52	3.97	4.21	4.35	3.72
M4	4.21	3.27	3.95	3.52	3.61	4.00	3.92	4.58	3.81	4.49	3.74
M5	3.19	3.09	3.28	4.94	3.03	3.37	3.60	3.69	3.51	3.39	3.52
M6	3.33	3.05	3.57	3.20	2.77	3.29	2.67	3.07	3.34	3.25	3.42
M7	2.30	3.51	1.74	1.76	2.23	1.84	1.69	2.45	2.22	1.94	1.82
M8	1.97	2.27	1.92	2.04	1.73	2.29	2.01	2.40	2.47	2.06	1.76
M9	2.58	2.33	2.01	2.17	2.12	2.57	2.13	2.42	2.54	2.11	2.45
M10	2.89	2.59	2.78	2.77	2.46	2.52	2.52	2.50	3.01	2.56	3.31
M11	2.55	2.50	2.89	2.53	2.55	2.19	2.63	2.33	2.34	2.43	2.54
M12	2.17	1.64	3.12	1.63	1.84	1.93	2.34	2.46	1.94	1.92	2.21
M13	2.18	2.26	2.39	2.31	2.61	2.50	2.93	2.25	2.56	3.45	3.06
M14	1.78	2.17	1.70	2.11	2.31	2.04	1.71	1.99	2.32	1.73	3.00
M15	2.24	2.34	1.75	1.74	2.78	1.86	3.40	3.07	1.86	2.04	1.80
M16	1.87	1.87	1.78	1.91	2.70	2.13	1.85	2.14	1.97	2.11	1.89
M17	1.68	1.63	1.60	2.08	1.92	2.82	1.65	1.78	2.14	1.81	1.86
M18	2.18	1.91	1.98	2.18	2.37	1.72	1.66	2.21	2.68	1.85	2.10
M19	2.08	1.84	1.81	1.81	2.30	1.77	1.85	2.51	1.75	2.52	2.90
M20	1.95	1.73	1.57	1.90	1.54	2.47	1.74	3.76	2.52	1.87	2.23
M21	1.57	1.66	3.09	1.74	1.65	1.77	1.99	1.87	3.70	2.22	2.04
M22	2.48	2.41	2.27	2.69	3.63	2.91	2.28	3.88	2.37	2.45	2.33
M23	2.28	2.28	2.96	2.32	2.59	2.33	2.56	2.16	2.23	3.13	2.71
M24	2.13	2.34	2.26	2.65	2.19	2.45	2.34	2.48	2.96	2.14	2.23
M25	2.08	2.08	2.58	2.73	2.60	2.21	2.64	2.28	2.57	2.02	2.74
M26	1.87	2.35	3.08	2.32	3.46	2.38	3.06	2.46	3.12	2.49	2.80

3.2.1 Performance comparison

The comparison results of performance predictions of the Bayesian regularisation neural network model and the HEC-HMS model for St. Marys can be found in Table 3. The performance predictions of the neural network model for Plover Mills are given in Table 4. The ANN model results for all datasets for both St. Marys and Plover Mills show that the Bayesian regularisation network offers more accurate flood flow values. The ANN model performances of St. Marys are also found superior compared to the HEC-HMS model. To provide for further comparison, the ANN simulated flood hydrograph is plotted in Figure 4 for St. Marys station. Finally, the improved flood output for St. Marys [obtained by equations (1) and (2)] is then used by the ANN2 model to update the computed HEC-HMS model flood flow value for the ungauged location Plover Mills [using equations (3) and (4)]. The improved output flood hydrograph for Plover Mills is plotted in Figure 5.

Figure 4 Improved flood hydrographs of test dataset for St. Marys station (Event June 2000) (see online version for colours)

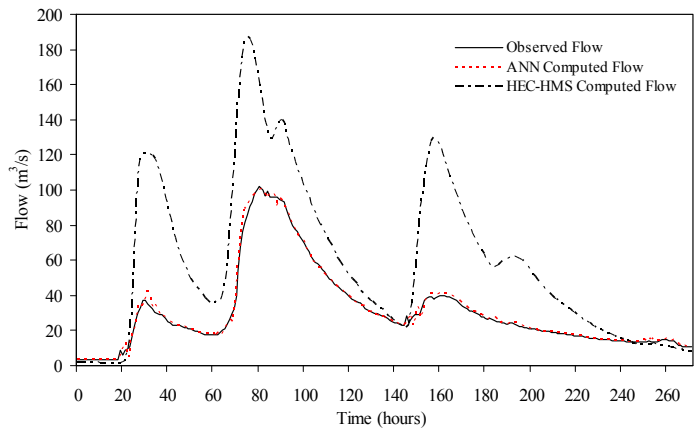

Figure 5 Improved flood hydrograph for the ungauged site, Plover Mills (Event June 2000) (see online version for colours)

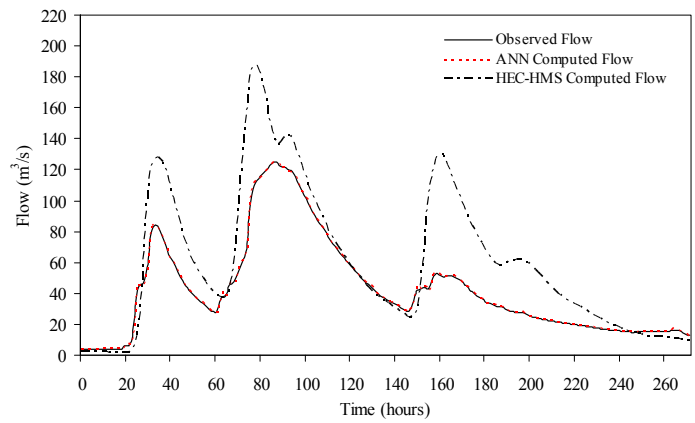

4 Results and discussions

The performance of ANN, assessed by the comparison of ANN model predictions and HEC-HMS model, is evaluated for only validation and test datasets. This evaluation is to determine the performance of the ANN model in simulating flood flow events for the ungauged sites. From Table 3 for St. Marys station, the ANN validation dataset presents the most accurate flood flow values with MAE = 0.763 m^3/s or FVE = –0.006; higher value of EI = 0.998; and smaller value of PFC = 0.076. The overall performance measures for the HEC-HMS model with the validation dataset are not as good: larger MAE = 25.173 m^3/s or value of FVE = –0.148; lower value of EI = 0.420 and higher value of PFC = 0.336 when compared to the ANN model. The ANN model performance for the test dataset is also superior. This can be seen from the comparison with the HEC-HMS model: lower value of MAE equal to 0.992 m^3/s opposed to a 28.608 m^3/s; slightly small FVE value of –0.010 against –0.895; very satisfactory ANN model with higher EI value of 0.995 against negative value of 1.844. In the latter case, the negative value of EI indicates that the output of the HEC-HMS model gives the more reliable mean of observed flood flow values; and slightly smaller value of PFC of 0.076 against 0.371. Furthermore, from Figure 4, the simulated flood hydrograph obtained using the ANN model is best matched by the observed flood hydrograph with the correlation coefficient value of 0.998 for the test dataset. The overall performance measures for validation and test datasets are also very good for Plover Mills ANN simulations, as given by Table 4. For example, in the case of validation dataset used with the ANN model, there is an optimal prediction of flood flow values with small MAE value of 0.343 m^3/s and very low FVE value of negative 0.002; a very satisfactory model performance with highest EI value of 1.000 and lower value of PFC equal to 0.036. These performance measures clearly indicate that the ANN model can be used to learn representations between the input variables and the output/target of the HEC-HMS computed flood flow at Plover Mills. For the test dataset, consisting of the improved flood flow at St. Marys, the performance prediction of the ANN model is also found to match observed flood flow better than the HEC-HMS computed flood flow. The ANN model is proven capable in mapping unknown input-output datasets with the EI and R values of 0.998 and 0.999 that are much higher than 0.595 and 0.888 of the HEC-HMS model, respectively. Finally, the high agreement is observed between the ANN simulated hydrograph and the observed flood hydrograph for Plover Mills station as shown in Figure 5.

5 Conclusions

This manuscript presents an output updating procedure based on the ANN approach. The overall performance measures (such as RMSE, FVE, MAE, EI, PFC, and R) of Bayesian regularisation ANN model are superior to the HEC-HMS hydrologic model for St. Marys station. Similarly, the performance results of all the statistical measures using training, validation and test datasets for Plover Mills station implies that the ANN model offers better prediction of the flood flow value for the ungauged site. For example, the ANN model shows the most accurate flood flow values with low values of RMSE and MAE, a better estimation of flow volume magnitude with smaller FVE value, satisfactory model EI value higher than a 0.995, a more accurate prediction of peak flow with lower value of PFC, and a value of R above 0.998. The results of analyses also show that the

implementation of Bayesian regularisation as the objective function in the network training using LM algorithm can provide a well generalised network for a given unknown input-output dataset. Furthermore, it has been shown that using additional meteorological data in the network training can considerably improve the trained network and result in a lower RMSE value. So, the Bayesian regularisation approach as the objective function in the ANN model using LM algorithm can successfully be applied to reduce the output flood flow of physically-based model. The improved flood flow(s) at the gauged streamflow location(s) can be subsequently used to improve the physically-based model computed flow value(s) at the ungauged location(s).

Acknowledgements

The authors would like to thank Universiti Teknologi Malaysia (UTM), the Ministry of Higher Education Malaysia (MOHE) and the University of Western Ontario, Canada for support of the presented research.

References

Abebe, A.J. and Price, R.K. (2004) 'Information theory and neural networks for managing uncertainty in flood routing', *Journal of Computing in Civil Engineering*, Vol. 18, No. 4, pp.373–380.

Abrahart, R.J. and See, L.M. (2007) 'Neural network modelling of non-linear hydrological relationships', *Journal of Earth System Science*, Vol. 11, No. 5, pp.1563–1579.

Ahmad, S. and Simonovic, S.P. (2005) 'An artificial neural network model for generating hydrograph from hydro-meteorological parameters', *Journal of Hydrology*, Vol. 315, Nos. 1–4, pp.236–251.

Anctil, F. and Rat, A. (2005) 'Evaluation of neural network streamflow forecasting on 47 watersheds', *Journal of Hydrology*, Vol. 10, No. 1, pp.85–88.

Anctil, F., Claude, M., Charles, P. and Vazken, A. (2004) 'A soil moisture index as an auxiliary ANN input for stream flow forecasting', *Journal of Hydrology*, Vol. 286, No. 1, pp.155–167.

Anctil, F., Perrin, C. and Andreassian, V. (2003) 'ANN output updating of lumped physically rainfall/runoff forecasting models', *Water Resources Bulletin*, Vol. 39, No. 5, pp.1269–1279.

ASCE Task Committee on Artificial Neural Networks in Hydrology (2000) 'Artificial neural networks in hydrology', *Journal of Hydrological Engineering*, Vol. 5, No. 2, pp.124–137.

Aytek, A., Asce, M. and Alp, M. (2008) 'An application of artificial intelligence for rainfall-runoff modeling', *Journal of Earth System Science*, Vol. 117, No. 2, pp.145–155.

Bertsekas, D.P. and Tsitsiklis, J.N. (1996) *Neuro-Dynamic Programming*, Athena Scientific, Belmont, Massachusetts, USA.

Beven, K.J. (2001) *Rainfall-Runoff Modelling*, The Primer, John Wiley and Sons, Chichester, UK.

Bhattacharya, B. and Solomatine, D.P. (2000) 'Application of neural networks in stage-discharge relationships', *Proc., 4th International Conference on Hydroinformatics*, Iowa City, USA.

Coulibaly, P., Anctil, F. and Bobée, B. (2001) 'Multivariate reservoir inflow forecasting using temporal neural networks', *Journal of Hydrologic Engineering*, Vol. 6, No. 5, pp.367–376.

Cullmann, J., Schmitz, G. and Gorner, W. (2006) *A New System for Online Flood Forecasting – Performance and Implications*, IHAR red book 303, Institute of Hydrology and Meteorology, University of Technology, Dresden, Germany.

Cunderlik, J.M. (2003) 'Hydrologic model selection for the CFCAS project: assessment of water resources risk and vulnerability to changing climatic condition', Water Resources Research Report No. 046, 38p, Department of Civil and Environmental Engineering, The University of Western Ontario, London, Ontario, Canada, ISBN: (print) 978-0-7714-2622-3; (online) 978-0-7714-2623-0.

Cunderlik, J.M. and Simonovic, S.P. (2004) 'Assessment of water resources risk and vulnerability to changing climatic conditions: calibration and verification data for the HEC-HMS hydrologic model', Report No. II, Department of Civil and Environmental Engineering, The University of Western Ontario, London, Ontario, Canada.

Eslamian, S.S., Gohari, A., Zareian M.J. and Firoozfar, A. (2012) 'Estimating Penman-Monteith reference evapotranspiration using artificial neural networks and genetic algorithm: a case study', *The Arabian Journal for Science and Engineering*, Vol. 37, No. 4, pp.935–944.

Foresee, F.D. and Hagan, M.T. (1997) 'Gauss-Newton approximation to Bayesian regularization', *Proc., International Joint Conference on Neural Networks*, Vol. 2, pp.1930–1935.

Goswami, M., O'Connor, K.M., Bhattarai, K.P. and Shamseldin, A.Y. (2005) 'Assessing the performance of eight real-time updating models and procedures for the Brosna River', *Journal of Earth System Science*, Vol. 9, No. 4, pp.394–411.

Govindaraju, R.S. and Rao, A.R. (2000) *Artificial Neural Networks in Hydrology*, Kluwer Academic Publisher, Dordrecht, The Netherlands.

Hagan, M.T. and Menhaj, M.B. (1994) 'Training feedforward networks with Marquardt algorithm', *IEEE Transactions on Neural Networks*, Vol. 5, No. 6, pp.989–993.

Iyer, M.S. and Rhinehart, R.R. (1999) 'A method to determine the required number of neural-network training repetitions', *IEEE Transactions on Neural Networks*, Vol. 10, No. 2, pp.427–432.

Jain, A. and Srinivasulu, S. (2006) 'Integrated approach to model decomposed flow hydrograph using artificial neural network and physically techniques', *Journal of Hydrology*, Vol. 317, Nos. 3–4, pp.291–306.

Lekkas, D.F., Onof, C., Lee, M.J. and Baltas, E.A. (2004) 'Application of artificial neural networks for flood forecasting', *Global Nest: The Int. Journal*, Vol. 6, No. 3, pp.205–211.

Liong, S-Y., Lim, W-H. and Paudyal, G.N. (2000) 'River stage forecasting in Bangladesh: neural network approach', *Journal of Computing in Civil Engineering*, Vol. 14, No. 1, pp.1–8.

MacKay, D.J.C. (1992) 'Bayesian interpolation', *Neural Computation*, Vol. 4, No. 3, pp.415–447.

Masters, T. (1995) *Advanced Algorithms for Neural Networks: A C++ Sourcebook*, John Wiley and Sons, New York, USA.

Moradkhani, H., Hsu, K-L., Gupta, H. and Sorooshian, S. (2004) 'Improved streamflow forecasting using self-organizing radial basis function artificial neural networks', *Journal of Hydrology*, Vol. 295, Nos. 1–4, pp.246–262.

Nash, J.E. and Sutcliffe, J.V. (1970) 'River flow forecasting through conceptual models: part I – a discussion of principles', *Journal of Hydrology*, Vol. 10, No. 3, pp.282–290.

Nguyen, D. and Widrow, B. (1990) 'Improving the learning speed of 2-layer neural networks by choosing initial values of the adaptive weights', *Proc., International Joint Conference on Neural Networks*, Vol. 3, pp.21–26.

Parent, A., Anctil, F., Cantin, V. and Boucher, M. (2008) 'Neural network input selection for hydrological forecasting affected by snowmelt', *Water Resources Bulletin*, Vol. 44, No. 3, pp.679–688.

Poff, N.L., Tokar, S. and Johnson, P. (1996) 'Stream hydrological and ecological responses to climate change assessed with an artificial neural network', *Limnology and Oceanography*, Vol. 41, No. 5, pp.857–863.

Prodanovic, P. and Simonovic, S.P. (2006) 'Assessment of risk and vulnerability to changing climatic conditions: inverse flood risk modelling of the Upper Thames River basin', Report No. VIII, Department of Civil and Environmental Engineering, The University of Western Ontario, London, Ontario, Canada.

Rajurkar, M.P., Kothyari, U.C. and Chaube, U.C. (2004) 'Modeling of the daily rainfall runoff relationship with artificial neural network', *Journal of Hydrology*, Vol. 285, No. 1, pp.96–113.

Tan, Y. and Van Cauwenberghe, A. (1999) 'Neural-network-based d-step-ahead predictors for nonlinear systems with time delay', *Engineering Applications of Artificial Intelligence*, Vol. 12, No. 1, pp.21–35.

Thirumalaiah, K. and Deo, M.C. (1998) 'River stage forecasting using artificial neural networks', *Journal of Hydrologic Engineering*, Vol. 3, No. 1, pp.26–32.

USACE (2000) *Hydrologic Modelling System HEC–HMS: Technical Reference Manual*, US Army Corps of Engineers, Hydrologic Engineering Center, Davis, California.

UTRCA (2009) *Inspiring a Healthy Environment: Flooding on the Thames River*, Upper Thames River Conservation Authority, London, Ontario, Canada, available at http://www.thamesriver.on.ca/Water_Management/flood_history.htm (accessed on 29 January 2010).

Wardah, T., Abu Bakar, S.H., Bardossy, A. and Maznorizan, M. (2008) 'Use of geostationary meteorological satellite images in convective rain estimation for flash-flood forecasting', *Journal of Hydrology*, Vol. 356, Nos. 3–4, pp.283–298.

Wilcox, I., Quinlan, C., Rogers, C., Troughton, M., McCallum, I., Quenneville, A., Heagy, E. and Dool, D. (1998) 'The Thames River basin: a background study for nomination under the Canadian Heritage Rivers system', Upper Thames River Conservation Authority, London, Ontario, Canada.

Xiong, L. and O'Connor, K.M. (2002) 'Comparison of four updating models for real-time river flow forecasting', *Hydrological Sciences Journal*, Vol. 47, No. 4, pp.621–639.

Xiong, L., O'Connor, K.M. and Guo, S. (2004) 'Comparison of three updating schemes using artificial neural network in flow forecasting', *Journal of Earth System Science*, Vol. 8, No. 2, pp.247–255.

Zealand, C.M., Burn, D.H. and Simonovic, S.P. (1999) 'Short-term streamflow forecasting using artificial neural networks', *Journal of Hydrology*, Vol. 214, Nos. 1–4, pp.32–48.